**Geomechanics and Engineering**, *Vol. 41, No. 2 (2025) 209-220*
https://doi.org/10.12989/gae.2025.41.2.209


# Experimental study on the pullout behavior of geogrid embedded in xanthan gum biopolymer-treated sand layers

Gi-Yun Kim[1a], Hwijae Lee[1b], Junghoon Kim[2c], Suhyuk Park[1d], Tae Sup Yun[2e] and Ilhan Chang*[1]

[1]*Department of Civil Systems Engineering, Ajou university, 206 World cup-ro, Yeongtong-gu, Suwon-si 16499, Republic of Korea*
[2]*Department of Civil and Environmental Engineering, Yonsei university, 50 Yonsei-ro, Seodaemun-gu, Seoul-si 03722, Republic of Korea*

(*Received November 26, 2024, Revised March 7, 2025, Accepted March 8, 2025*)

**Abstract.** Geogrid pullout is a critical failure mode in mechanically stabilized earth (MSE) walls and must be thoroughly assessed to ensure stability. Pullout resistance consists of skin friction between the soil and geogrid and bearing (passive) resistance generated by the transverse ribs. Due to the nonlinear and complex soil–geogrid interactions, pullout tests are recommended by design and construction guidelines. This study examined the potential of encapsulating geogrids within a biopolymer-based soil treatment (BPST) layer to enhance pullout resistance. Laboratory pullout tests, conducted using an independently developed apparatus, assessed geogrid performance encapsulated in xanthan gum biopolymer hydrogel under initial (wet) and dehydration (dry) conditions across varying normal pressure levels. Results showed that under the initial (wet) condition, pullout resistance increased by at least 10% at low normal pressure levels (≤50 kPa) due to improved adhesion. Under dehydration (dry) conditions, pullout resistance significantly increased, exceeding the geogrid's tensile strength at low normal pressure levels (25 kPa), attributed to enhanced bonding and particle–geogrid interlocking. The apparent friction coefficient and interaction coefficient ratio (ICR) were introduced as metrics to evaluate pullout resistance performance. The BPST method proved effective in addressing challenges where compaction is unsuitable, reinforcement length is constrained in narrow backfill areas, or fine-grained soils are required. This eco-friendly method provides a sustainable alternative for MSE wall applications, offering improved mechanical performance and versatility.

**Keywords:** Biopolymer-based soil treatment (BPST); geogrid; pullout resistance; soil-geogrid interaction

## 1. Introduction

A geogrid is a type of geosynthetic ground reinforcement material that is often utilized in geotechnical engineering applications such as mechanically stabilized earth (MSE) walls, soil slopes, embankments, pavements, and foundation constructions (Wang *et al*. 2016, Wang *et al*. 2023, Zamani *et al*. 2023, Abdi *et al*. 2024). Geogrid-reinforced soil structures minimize soil mass deformation during construction and improve tensile strength, thereby enhancing the bearing capacity and earthwork stability (Wang *et al*. 2023, Aregbesola and Byun 2024). Fig. 1 shows typical consideration cases for assessing the internal stability of MSE walls reinforced with a geogrid. A horizontally placed geogrid supports an active wedge on one side and is anchored to a stable reinforced zone on the other side

The behavior of MSE walls reinforced with geogrids is commonly governed by the interactions that develop between the geogrid and the backfill soil. The primary function of geogrid reinforcement is to redistribute stress within the soil mass, improving the internal stability of reinforced soil structures. The stress redistribution within a reinforced soil mass and the structural deformation response are determined by the shear strength, geogrid tensile properties, and stress transfer mechanisms between the soil and geogrid. Pullout tests have been adopted to provide valuable information for analyzing stress transfer mechanisms; however, further understanding of the behavior mechanisms that develop during pullout testing is required. Therefore, a stable and economic soil reinforcement design requires a comprehensive understanding of soil-reinforcement interaction mechanisms (Teixeira *et al*. 2007, Abdi and Arjomand 2011).

Failure may develop along the potential slip planes in geogrid-reinforced structures (Fig. 1). The interaction between a geogrid and the surrounding soil is simplified such that the soil sliding over the geogrid is related to direct shear, with the geogrid anchored in the passive zone being pulled out owing to the lateral movement of the soil. This approach has been commonly adopted in studying interface

*Corresponding author, Associate Professor
E-mail: ilhanchang@ajou.ac.kr
[a]Graduate Student
E-mail: kky950317@ajou.ac.kr
[b]Graduate Student
E-mail: alex060615@ajou.ac.kr
[c]Graduate Student
E-mail: kjh00005@yonsei.ac.kr
[d]Graduate Student
E-mail: phy9958@ajou.ac.kr
[e]Professor
E-mail: taesup@yonsei.ac.kr



ISSN: 2005-307X (Print), 2092-6219 (Online)

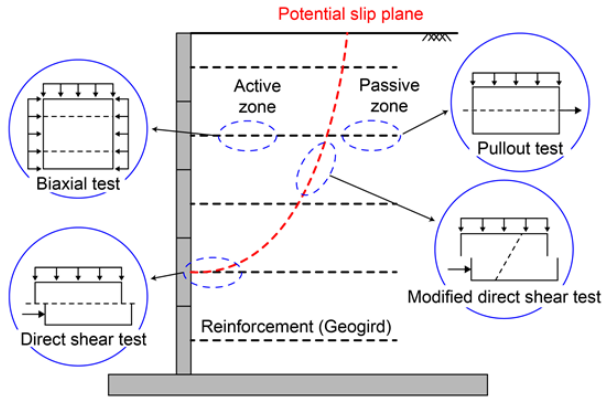


Fig. 1 Schematic diagram of tests used to investigate soil-geogrid interaction behavior mechanisms (based on Palmeira 2009, Moraci *et al*. 2014)

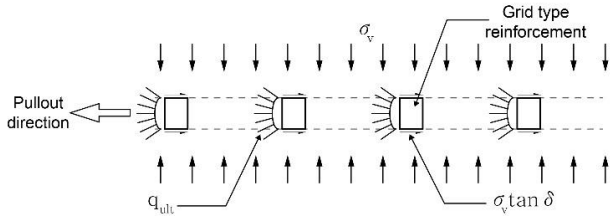


Fig. 2 Pullout resistance mechanisms of a grid-type reinforcement (based on Sieira *et al*. 2009, Mirzaalimohammadi *et al*. 2019)

behavior (Abdi and Arjomand 2011, Derksen *et al*. 2021). One of the most significant failure types in geogrid reinforcement is the geogrid pulled out from the soil, which should be considered when assessing the design and internal stability of reinforced soil structures.

The pullout test for geogrids embedded in backfill is a prerequisite for MSE wall design (Berg *et al*. 2009a, Berg *et al*. 2009b). The pullout resistance is primarily determined by the backfill properties, geometrical and mechanical properties of the geogrid, and normal stress, resulting in a nonlinear and complex relationship between the geogrid and the surrounding soil (Pant and Ramana 2022). Among the common experimental approaches, the laboratory pullout test is regarded as the most reliable and effective approach for analyzing the geogrid–soil interaction behavior (Wang *et al*. 2023). The main interaction mechanisms that determine the geogrid pullout resistance include skin friction between the soil and the reinforced solid surface as well as the bearing resistance against transverse members (Moraci and Gioffrè 2006, Palmeira 2009, Moraci *et al*. 2014, Cardile *et al*. 2017). Therefore, the pullout resistance of a geogrid is commonly regarded as the sum of the skin friction (interface shear) and bearing (passive) resistance components (Jewell 1996) (Fig. 2). ASTM D6706 (2021) provides a general outline for laboratory testing that is regarded as a reliable approach for geogrid behavior assessment (Pant and Ramana 2022).

Several studies have been performed to investigate the failure mechanisms and improve the pullout resistance of geogrid-reinforced structures: 1) geogrid type and shape (Bergado *et al*. 1987, Khedkar and Mandal 2009, Horpibulsuk and Niramitkornburee 2010, Wang *et al*. 2016, Pant *et al*. 2019, Bhowmik *et al*. 2023); 2) different backfill soil types (Abdi and Zandieh 2014, Mirzaeifar *et al*. 2022); 3) attachments on geogrids (e.g., bearing element) (Esfandiari and Selamat 2012, Hataf and Sadr 2015, Sadat Taghavi and Mosallanezhad 2017, Maleki *et al*. 2021, Abdi *et al*. 2022), and 4) biocementation around geogrid member (Gao *et al*. 2021). These studies focused on the impact of numerous parameters on the geogrid response under pullout loads, providing valuable information for constructing reinforced soil structures with geogrids (Wang *et al*. 2016).

The current MSE wall design guidelines recommend using granular materials with sufficient drainage and strength as backfill materials while cautioning against the excessive use of fine-grained soils (Ghasemi *et al*. 2024). However, in practice, engineers often choose locally available fine-grained soils to reduce environmental impacts such as limited granular material availability, transportation costs and carbon footprint, shortened construction timelines, new aggregate extraction, and local soil disposal (Christopher and Stulgis 2005, Yang *et al*. 2019, Razeghi and Ensani 2023, Ghasemi *et al*. 2024). Fine-grained soils are the most abundant and cheap materials for construction, but their low frictional resistance at the soil-reinforcement interface can lead to reinforcement pullout, affecting the stability of MSE walls (Abdi and Arjomand 2011, Abdi and Zandieh 2014, Ghasemi *et al*. 2024). Shear failure at the interface can be induced by high shear stresses near the reinforcement, which decreases rapidly with growth away from it. If the backfill soil does not satisfy the geotechnical requirements, it is desirable to place a thin layer of high-strength granular soil around the reinforcement (Abdi *et al*. 2009). The "sandwich technique" or "sand-cushion" approach may effectively address the problem of employing poor-quality backfill by increasing the stress transfer mechanism owing to interface properties (Abdi *et al*. 2009, Abdi and Arjomand 2011, Abdi and Zandieh 2014, Ghasemi *et al*. 2024).

If the properties of locally available soils are insufficient for geotechnical requirements, chemical additions are utilized to improve engineering performance. Conventional soil improvement agents like cement, lime, and fly ash adversely affect the environment and contribute to climate change via $CO_2$ emissions. Meanwhile, biopolymer-based soil treatment (BPST) is actively considered to be a new binding material in geotechnical engineering (Chang *et al*. 2019b, Chang *et al*. 2020, Choi *et al*. 2020, Jain *et al*. 2023). Biopolymers, which are eco-friendly and sustainable materials, serve as soil treatment and ground-improvement binders. Drying, accompanied by biopolymer hydrogel dehydration, improves BPST shear strength through soil surface coating and inter-particle bridging induced by biopolymer biofilm condensation (Chang *et al*. 2016a, Lee *et al*. 2017, Chang *et al*. 2020). Xanthan gum biopolymer (XG) is used as gelling and suspending agents for viscosity control in various industries, including oil and food, owing to their sufficient stability in terms of temperature, pH, electrolyte concentrations, and compatibility with food additives (Becker *et al*. 1998, Garcıa-Ochoa *et al*. 2000, Chang *et al*. 2015a, Chang *et al*. 2020). Motivated by the

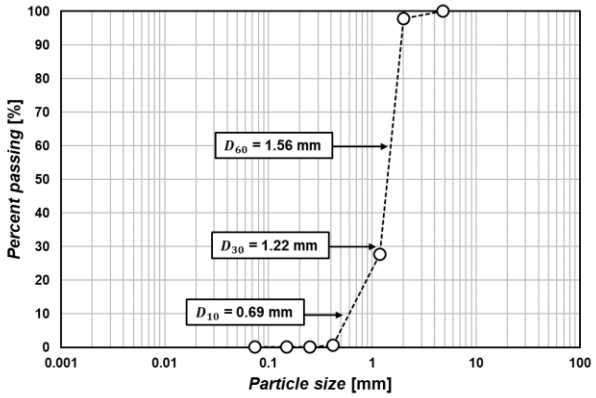


Fig. 3 Particle size distribution of Jumunjin sand

previous research approach known as the "sandwich technique" or "sand-cushion", the strength development mechanism of BPST is intended to improve the interaction engineering performance between backfill soil and geogrid. The XG-BPST method can ensure engineering efficiency while satisfying environmental protection regulations and carbon neutrality; however, further investigation is required to determine the suitability, durability, constructability, and economic feasibility of a construction site (Chang *et al*. 2020).

This study proposes an innovative concept that uses XG-BPST to improve the mechanical behavior of reinforced soil structures. Laboratory tests were performed on specimens reinforced with geogrids encapsulated in a thin layer of XG-BPST in sandy soil to assess their feasibility. The XG-BPST system improved the interface shear strength by effectively bonding the soil and geogrid, making it more difficult to pull the geogrid out of the soil. The proposed XG BPST-geogrid system aims to address the following geotechnical challenges:

- When the site is unsuitable for compaction, and it is impossible to obtain an adequate reinforcing length under narrow backfill conditions.
- The trend of using local cohesive soils as construction materials to decrease negative environmental effects and costs associated with aggregate extraction.
- Increasing demand for eco-friendly and sustainable soil treatment techniques due to environmental issues about conventional chemical additions (i.e., lime or cement).

## 2. Materials

### *2.1 Soil*

Jumunjin sand, which is granular soil with high sphericity and low fine-grained content (USCS = SP), was used in this study (Fig. 3). Physical properties and shear strength parameters of Jumunjin sand are summarized in Table 1. The shear strength parameters presented in Table 1 were determined using a direct shear test (ASTM D3080 (2012)) under the same unit weight condition (17.4 kN/m³) that was also applied during the geogrid pullout tests.

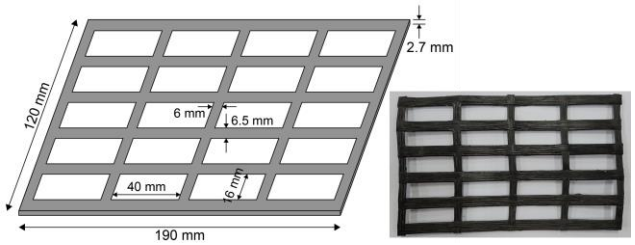


Fig. 4 Geometric dimensions of the geogrid used in this study

Table 1 Physical properties and shear strength parameters of Jumunjin sand

| Category | Unit | Test result |
|---|---|---|
| USCS | | SP |
| $C_u$ / $C_c$ | mm | 2.3 / 1.4 |
| Specific gravity | | 2.65 |
| Maximum dry unit weight | kN/m$^3$ | 18.1 |
| Minimum dry unit weight | kN/m$^3$ | 14.4 |
| Dry unit weight of the test | kN/m$^3$ | 17.4 |
| Relative density | % | 84.3 (Dense) |
| Internal friction angle | ° | 38.4 |
| Cohesion | kPa | 0 |

### *2.2 Geogrid*

The biaxial geogrid used in this study was manufactured from high-strength, low-elongation polyester coated with PVC (Polyvinyl Chloride). The tensile strength of the geogrid is 40 kN/m, and Fig. 4 indicates its geometric dimensions. The geogrid has a rectangular mesh configuration with internal openings measuring 40 mm × 16 mm, and the apertures comprise 56% of the total area.

### *2.3 Xanthan gum biopolymer (XG)*

BPST utilizes biopolymers produced in an exo-cultivation facility, enabling precise control over both their quantity and quality (Chang *et al*. 2020). Moreover, directly mixing biopolymers with soil forms a uniform biopolymer-treated soil mixture, offering immediate reinforcement through the formation of an electrostatic biopolymer–soil matrix (Chang and Cho 2012, Chang *et al*. 2016a, Chang and Cho 2019, Chang *et al*. 2019a, Chang *et al*. 2020).

In this study, a purified XG (Sigma-Aldrich, CAS No. 11138-66-2) was used to improve the pullout resistance of the geogrid. The XG was dissolved in deionized water to form a hydrogel solution, which was then mixed with sand to form a XG–sand mixture (hereafter, XG-BPST). To prepare the XG-BPST samples, the mixing ratio of deionized water and XG was determined based on the target biopolymer to sand ratio in mass ($m_b/m_s$). Mechanical properties and pullout tests on XG-BPST samples were performed under initial (wet) or dehydration (dry) conditions after 1 week of curing at room temperature (25°C). Fully dehydrated XG-BPST samples, which exhibited the highest strength, had a water content of less than 2%.

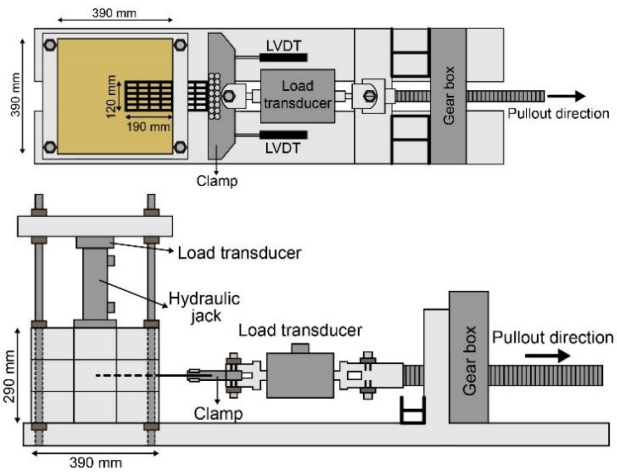


Fig. 5 Schematic diagram of the pullout test apparatus

## 3. Experimental program

### *3.1 Pullout test apparatus*

ASTM D6706 (2021) recommends that the minimum width of the pullout box be 20 times $D_{85}$ or 6 times the maximum soil particle size, with a minimum length of at least 5 times the maximum geosynthetic aperture size. The pullout box above and below the geosynthetic has a depth of at least 6 times $D_{85}$ or 3 times the maximum soil particle size, whichever is greater. The dimensions of the independently developed pullout box used in this study were 390 mm in length, 390 mm in width, and 290 mm in height (Fig. 5), which satisfy the minimum requirements provided by ASTM D6706 (2021), considering the maximum particle size and geogrid aperture of 2 mm and 40 mm, respectively.

The pullout test apparatus comprised a pullout box constructed from 15 mm thick steel plates, a normal pressure application device, a horizontal pulling mechanism, and a data acquisition system for monitoring forces and displacements. To reduce adhesion and friction between the soil and the pullout box sidewalls, ASTM D6706 (2021) recommends applying non-adhesive grease to the inner surfaces of the pullout box, followed by covering them with polyethylene sheets. A slit measuring 10 mm in height and 130 mm in width was included in the center of the front wall to facilitate the geogrid pullout from the confined soil box.

To apply normal confinement to the soil specimen, a hydraulic jack was connected to a rigid steel plate that covered the entire area of the pullout box, with the top boundary acting as a rigid boundary. The normal pressure transmitted by the hydraulic jack was measured using a load transducer (DSCK-10T, Bongshin Co., Ltd.) positioned between the hydraulic jack and the reaction beam. The surcharge pressure applied to the embedded geogrid was the combined effect of the soil weight above the geogrid and the direct normal pressure applied to the soil specimen. Throughout the testing, these systems ensured constant confining pressure on the embedded geogrid.

The geogrid part embedded in the confined pullout box, was secured at one end using steel screws passed through its apertures into a clamp with multiple holes. A rubber plate was placed between the geogrid and the clamp to minimize relative movement during the pullout process. The clamp was connected to a load transducer (TRC-3T, Bongshin Co., Ltd.) to measure the pullout force and to a gearbox (D.C. geared motor, Myungsung Electric Co., Ltd.) to facilitate the geogrid pullout. The gearbox was operated using a speed controller, and the test was conducted under displacement-controlled conditions, pulling the geogrid at a consistent displacement rate. To monitor the frontal displacement of the geogrid, linear variable differential transformers (LVDTs; CDP-100, Tokyo Sokki Kenkyujo (TSK) Co., Ltd.) were attached to the clamp. All instruments used in the laboratory tests were calibrated prior to the experiments.

### *3.2 Test conditions*

Pullout tests were conducted on geogrids encapsulated with a thin layer of XG-BPST within a pullout box. A 20 mm thick XG-BPST layer was applied at the center of the box to ensure both workability and economic efficiency. As part of a feasibility study investigating the enhancement of pullout resistance in encapsulated geogrids, two concentrations of XG hydrogel solution were determined, considering both initial (wet) and dehydration (dry) conditions. Furthermore, MSE walls that are greater than 5 m in height were subjected to normal pressures within 100 kPa; then normal pressures of 25, 50, and 100 kPa were determined to simulate pullout at different elevations of the wall. The test conditions used in this study are detailed in Table 2.

Direct shear tests on XG-BPST were conducted at a dry unit weight of 17.4 kN/m³, with the results presented in Fig. 6. Under the initial (wet) XG-BPST condition, the internal friction angle showed minimal variation, while a slight increase in cohesion was observed, resulting in a modest improvement in shear strength. However, as the $m_b/m_s$ ratio increased under dehydration (dry) conditions, cohesion experienced a significant rise due to interparticle bridging, leading to a substantial enhancement in soil shear strength (Lee *et al*. 2023b).

### *3.3 Laboratory test procedure*

The backfill soil for MSE walls requires dense compaction; hence, the model ground was compacted in five stages. Each layer was compacted 10 times using a 4.5 kg rammer to achieve a relative density of 84.3%. One end of the geogrid was secured to a clamp and embedded in the pullout box, with an embedded section measuring 190 mm in length and 120 mm in width. During the formation of the model ground, XG-BPST samples were prepared, and the geogrid was encapsulated within the center of a 20 mm thick XG-BPST layer, as depicted in Fig. 7.

The pullout tests were conducted under both initial (wet) and dehydration (dry) conditions, determined by the state of the hydrogel. The test for the initial (wet) condition was performed immediately after forming the model ground,

Table 2 Summary of laboratory test variables

| Case | XG treated ratio (UT / XG) | Water content [%] | XG hydrogel state (W / D) | Normal pressure [kPa] (N25 / N50 / N100) | Test name | Symbol |
|---|---|---|---|---|---|---|
| 1 | Untreated (UT) | - | - | 25 | UT-N25 | ○ |
| 2 | | | | 50 | UT-N50 | |
| 3 | | | | 100 | UT-N100 | |
| 4 | XG treated $m_b/m_s$ = 0.5% (XG0.5) | 10 | Wet (W) | 25 | XG0.5(W)-N25 | △ |
| 5 | | | | 50 | XG0.5(W)-N50 | |
| 6 | | | | 100 | XG0.5(W)-N100 | |
| 7 | | | Dry (D) | 25 | XG0.5(D)-N25 | |
| 8 | XG treated $m_b/m_s$ = 1.0% (XG1.0) | | Wet (W) | 25 | XG1.0(W)-N25 | □ |
| 9 | | | | 50 | XG1.0(W)-N50 | |
| 10 | | | | 100 | XG1.0(W)-N100 | |
| 11 | | | Dry (D) | 25 | XG1.0(D)-N25 | |

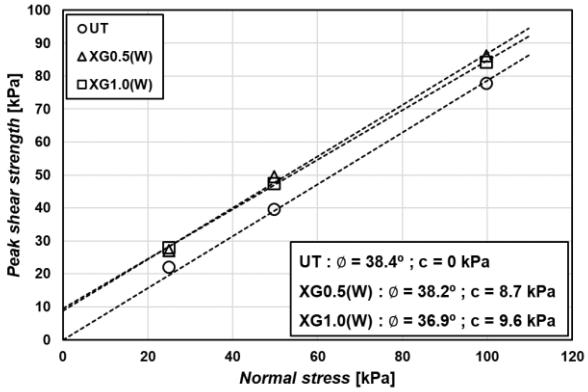


(a) Initial (wet) conditions

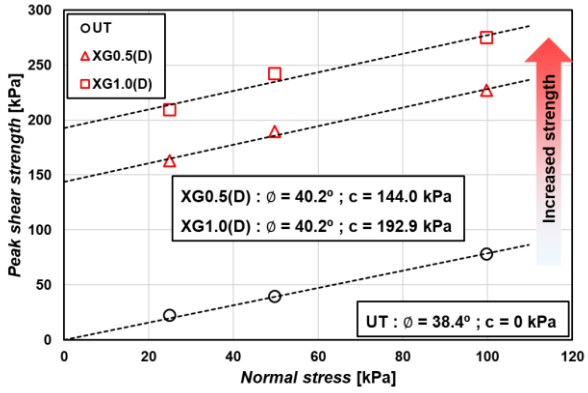


(b) Dehydration (dry) conditions

Fig. 6 Shear strength parameters based on direct shear test

while the test for the dehydration (dry) condition was performed after curing the specimen for one week at room temperature (25°C). The upper portion of the XG-BPST layer was filled using the same compaction process as the rest of the model ground. To ensure uniformly distributed normal pressure on the soil, a steel plate was placed on top of the specimen.

A hydraulic jack was employed to apply normal pressures of 25, 50, and 100 kPa for the tests. Each normal pressure was maintained for 30 minutes, allowing the

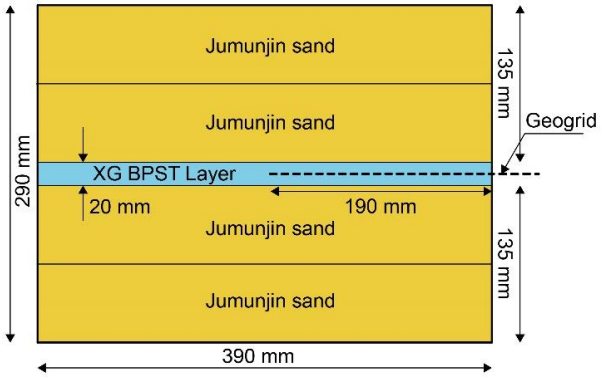


Fig. 7 Composition of the geogrid encapsulated with XG-BPST layer within pullout box

vertical deformations of the soil specimen to stabilize and become negligible before initiating the pullout process. Following the application of confinement, the geogrid encapsulated within the XG-BPST layer was positioned to align with the level of the slit in the pullout box.

The geogrid pullout tests were conducted using a displacement-controlled method, with a horizontal displacement rate of 1 mm/min, following ASTM D6706 (2021). During the pullout process, an automated data acquisition system (SSW-50D, TSK Co., Ltd.) continuously recorded the pullout force, clamp displacement, and normal pressure. The tests were terminated when the clamp displacement reached 70 mm or when the geogrid ruptured. To ensure the reliability and repeatability of the results, more than three tests were performed under identical conditions.

## 4. Test results

### *4.1 Interface shear strength parameters at pullout*

The pullout test provides data on the pullout force corresponding to pullout displacement for each normal confinement condition, as summarized in Table 3. The interface shear stress at the soil-geogrid contact surface can

Table 3 Pullout test results based on the normal confinement conditions

| Pullout Displacement [mm] | Pullout force [kN/m] | | | | | | | | | | |
|---|---|---|---|---|---|---|---|---|---|---|---|
| | UT | | | XG0.5(W) | | | XG0.5(D) | XG1.0(W) | | | XG1.0(D) |
| | N25 | N50 | N100 | N25 | N50 | N100 | N25 | N25 | N50 | N100 | N25 |
| 0 | 0 | 0 | 0 | 0 | 0 | 0 | 0 | 0 | 0 | 0 | 0 |
| 2 | 3.68 | 3.36 | 3.71 | 3.01 | 3.23 | 4.75 | 3.51 | 5.71 | 3.94 | 3.51 | 2.89 |
| 4 | 7.58 | 7.58 | 7.42 | 5.45 | 6.28 | 10.72 | 4.93 | 10.12 | 7.05 | 7.57 | 5.79 |
| 6 | 11.91 | 11.69 | 14.23 | 8.09 | 10.20 | 14.06 | 8.47 | 11.94 | 11.48 | 11.08 | 9.26 |
| 8 | 11.91 | 14.83 | 20.72 | 11.47 | 14.45 | 19.36 | 11.52 | 15.05 | 15.41 | 17.39 | 15.34 |
| 10 | 12.13 | 17.00 | 25.98 | 13.54 | 16.54 | 24.16 | 15.44 | 16.09 | 19.12 | 22.45 | 19.97 |
| 12 | 14.07 | 18.30 | 30.62 | 15.23 | 18.92 | 26.57 | 19.26 | 18.17 | 21.52 | 26.28 | 24.32 |
| 14 | 14.51 | 18.51 | 32.48 | 15.99 | 20.50 | 29.05 | 23.02 | 18.43 | 22.96 | 29.11 | 26.92 |
| 16 | 13.86 | 19.25 | 34.33 | 16.93 | 21.13 | 31.93 | 26.02 | 18.95 | 24.21 | 29.57 | 30.97 |
| 18 | 13.21 | 18.30 | 35.57 | 17.30 | 21.41 | 32.11 | 29.15 | 19.21 | 24.35 | 30.25 | 33.29 |
| 20 | 11.26 | 17.96 | 36.19 | 17.68 | 22.05 | 33.77 | 32.41 | 18.17 | 24.32 | 31.04 | 36.47 |
| 22 | 11.04 | 16.46 | 35.26 | 18.05 | 23.05 | 32.99 | 34.89 | 17.39 | 23.85 | 30.60 | 38.21 |
| 24 | 9.96 | 15.91 | 34.64 | 16.55 | 21.23 | 32.18 | 36.50 | 16.35 | 22.74 | 29.83 | 41.11 |
| 26 | 8.66 | 13.10 | 33.10 | 16.36 | 19.70 | 31.20 | 38.97 | 15.31 | 21.57 | 29.16 | 42.26 |
| 28 | 7.58 | 12.77 | 30.31 | 16.36 | 19.53 | 30.91 | 40.76 | 13.24 | 20.05 | 27.68 | 43.42 |
| 30 | 7.36 | 11.26 | 28.77 | 15.42 | 17.76 | 28.55 | | 11.94 | 19.50 | 26.18 | |
| 32 | 6.28 | 10.39 | 27.84 | 14.86 | 15.39 | 26.97 | | 11.42 | 17.96 | 23.71 | |
| 34 | 5.41 | 8.44 | 24.44 | 12.41 | 14.36 | 24.64 | - | 10.64 | 15.85 | 23.22 | - |
| 36 | 4.76 | 7.90 | 20.41 | 11.66 | 12.41 | 21.40 | | 10.38 | 14.51 | 17.19 | |
| 38 | 4.76 | 6.60 | 19.18 | 10.16 | 10.12 | 18.40 | | 9.08 | 13.00 | 16.24 | |
| 40 | 2.38 | 6.06 | 18.87 | 9.97 | 8.84 | 16.32 | | 8.57 | 10.55 | 13.30 | |

be determined using two widely used procedures: i) the mobilizing process method and ii) average resistance method. The average resistance method is often used as it simplifies the calculation by averaging stress over the contact surface. This approach aligns with the design principles for most reinforced soil structures, which are based on the limit equilibrium method (Ochiai *et al*. 1996).

The average resistance method is further divided into three types based on how the average value is calculated: the total area, effective area, and maximum slope methods. In this study, the total area method was employed because it provides conservative (safest) estimates and allows straightforward analysis by measuring the displacement of the geogrid front during testing. This method is also advantageous as it can effectively assess pullout force regardless of the geogrid tensile strength distribution (Shin and Yun 2003). Assuming that frictional forces are uniformly distributed above and below the geogrid, the interface shear stress (τ) can be calculated using the following equation

$$\tau = \frac{P}{2L} \tag{1}$$

Where $P$ (kN/m) is the pullout force (per unit width), and $L$ (m) is the length of the geogrid that resists pullout.

Fig. 8 and Table 3 present the geogrid pullout test results for both untreated and XG-BPST conditions. In the early stage of pullout, the pullout resistance increased linearly, irrespective of the applied normal pressure. As the pullout process progressed, the geogrid started to move relative to the surrounding soil, leading to a progressive extraction of the geogrid from the ground. As pullout displacement increased, the rate of pullout resistance growth slowed, eventually reaching a nonlinear peak, marking the failure point. Beyond this peak, the pullout resistance decreased nonlinearly until it stabilized at the residual pullout resistance level.

The pullout force increased with higher normal pressures because the soil surrounding the geogrid experienced greater confinement under these conditions. The geogrid pullout resistance is influenced by several factors, including skin friction along the soil and geogrid interfaces, soil–soil shear strength at the apertures, and bearing (passive) resistance mobilized in front of the transverse ribs. These factors contribute to the peak pullout resistance and the displacement behavior observed during testing.

Under the initial (wet) condition, XG hydrogel reduces the frictional resistance of sand, as shown in Fig. 6, due to its pseudo-plastic properties (Stokes *et al*. 2011, Lee *et al*. 2023b). When the geogrid was encapsulated in this wet condition at low normal pressure levels (≤50 kPa), it exhibited higher pullout resistance compared to the untreated condition. This improvement is attributed to the enhanced adhesion between the geogrid and the surrounding soil provided by the XG hydrogel (Lee *et al*. 2017). However, at higher normal pressure levels (100 kPa), the lubricating effect of the XG hydrogel reduced the interface friction of the soil surrounding the geogrid under the confined pressure, weakening the interlocking effect

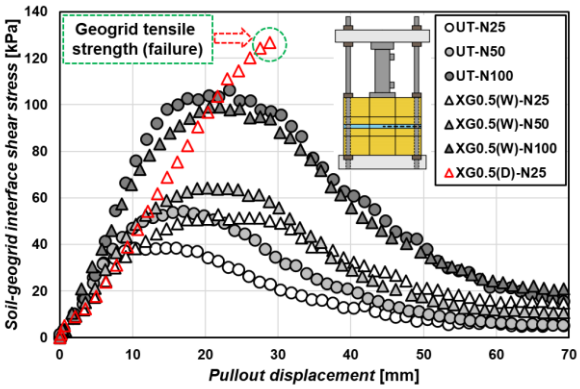


(a) 0.5% $m_b/m_s$ XG-BPST condition

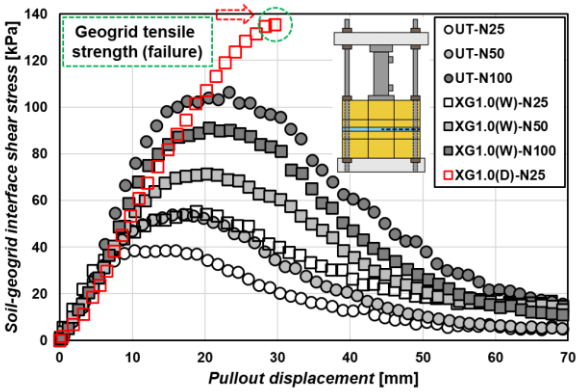


(b) 1.0% $m_b/m_s$ XG-BPST condition

Fig. 8 Shear strength developing at the soil-geogrid contact surface during geogrid pullout

(Lee *et al*. 2021). Consequently, the bearing (passive) resistance also decreased while this reduction in bearing resistance was relatively minor compared to the untreated condition.

In contrast, under the dehydration (dry) condition, XG-BPST demonstrated its effectiveness in significantly improving geogrid pullout resistance. This improvement is attributed to the ability of BPST to bind the soil particles around the geogrid, thereby enhancing particle–geogrid interlocking. Moreover, the anchoring effect of the sand surrounding the encapsulated geogrid layer further restricted its relative movement, thereby enhancing the geogrid resistance to pullout forces. The XG-BPST layer anchored the geogrid, preventing it from being pulled out, and pullout displacement developed because of geogrid tensile strain. The accumulating tensile strain led the geogrid rib to gradually rupture and then broke entirely. It demonstrated almost three times more pullout resistance than the untreated condition at the identical confined pressure. Following the construction of the MSE walls, the XG-BPST will progressively evaporate water, and the bonding properties of XG will develop, improving geogrid pullout resistance and wall stability. For XG-BPST under dehydration (dry) conditions, geogrid rupture occurred at the lowest normal pressure of 25 kPa; hence, tests at higher normal pressures were not performed.

Fig. 9 indicates the relationship between peak interface shear stresses and different normal confinement pressures,

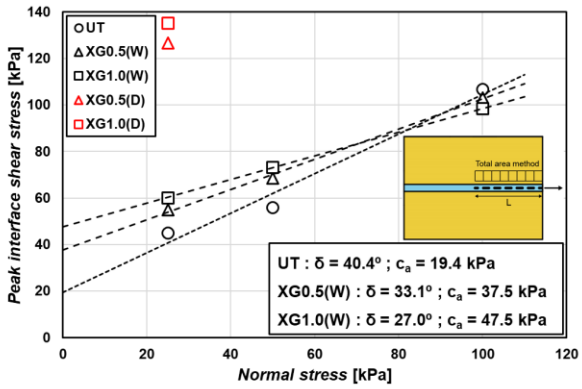


Fig. 9 Soil-geogrid peak interface shear stress linear relationship using the total area method

along with the interface shear strength parameters (adhesion, $c_a$; average interface friction angles, $\delta$) for each test condition. As previously noted, skin friction and bearing resistance contribute to the soil–geogrid interface shear strength. However, under the initial (wet) condition, the lubricating effect of the XG hydrogel reduced the average interface friction angle. Despite this, at normal stress levels below 80 kPa, the XG hydrogel enhanced shear strength through increased adhesion, resulting in an overall improvement in interface shear stress behavior compared to the untreated condition, which involved cohesionless soil. These findings highlight that XG-BPST effectively enhances soil–geogrid interaction under normal stress levels below 80 kPa, corroborating the results observed in Fig. 8.

### *4.2 Apparent friction coefficient and interaction coefficient ratio between soil and geogrid*

The apparent friction coefficient is a comprehensive strength parameter that represents the combined effects of friction and interaction between the soil and the geogrid. Unlike the traditional friction coefficient, which is determined solely by the internal friction angle of the soil, the apparent friction coefficient ($f$) accounts for the overall interface behavior. It is defined as the ratio of the interface shear strength ($\tau$) to the corresponding normal pressure ($\sigma_n$) (Namjoo *et al*. 2021).

$$f = \frac{\tau}{\sigma_n} \tag{2}$$

$f$ provides a more holistic understanding of the soil–geogrid interaction, encompassing both frictional and adhesive components of the interface shear strength. According to previous studies, soil dilatancy at the interface significantly affects pullout resistance and the $f$ of the interface (Moraci and Gioffrè 2006).

Fig. 10 shows the variation in the apparent friction coefficient of the geogrid encapsulated with XG-BPST as a function of the applied normal pressure. The results indicate that the apparent friction coefficient of the mobilized peak pullout interface decreases with increasing normal pressure. This phenomenon, also reported by Moraci and Recalcati (2006), can be attributed to two key factors:

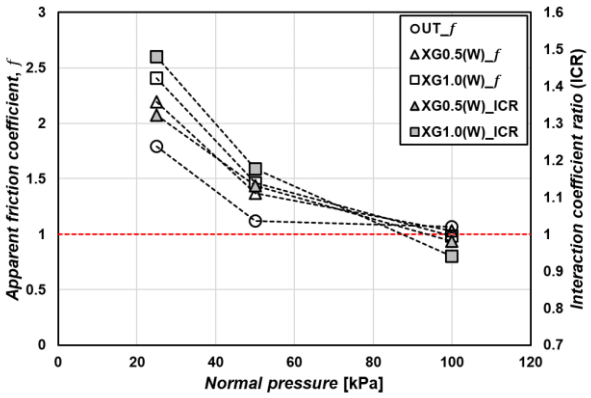


Fig. 10 Apparent friction coefficient ($f$) and interaction coefficient ratio (ICR) by normal pressure based on the pullout test

1) Soil Dilatancy: As normal pressure increases, the local pressure rises due to the energy required to expand the dilatancy surface at each level of normal pressure. Moreover, the stiffness of the surrounding soil restricts this dilatancy, a condition referred to as "confined dilatancy," further influencing the interface behavior.
2) Interface Tangential Stress Distribution: A secondary, less intense phenomenon occurs due to changes in the tangential stress distribution along the interface. These changes, along with the geogrid's extensibility, affect the pullout strength and contribute to the observed decrease in the apparent friction coefficient.

These factors combined explain the observed trend in the apparent friction coefficient under varying normal pressures (Moraci and Recalcati 2006, Moraci and Gioffrè 2006).

The apparent friction coefficient decreases with increasing normal pressure because, at low normal pressures, sand particles can rearrange and dilate more easily, contributing to higher interface shear strength relative to the normal pressure. In contrast, at high normal pressures, the rearrangement and dilation of sand particles are suppressed, reducing the relative contribution of these mechanisms to the interface shear strength.

The interaction coefficient ratio (ICR) can be used to assess the improvement in interaction between various reinforcement systems in pullout mechanisms. According to Sadat Taghavi and Mosallanezhad (2017), the interface shear strength $\tau_f$ may be determined using the following equation

$$\tau_f = c_a + \sigma_n tan\delta \quad (3)$$

To compare the improved effect of XG-BPST to the untreated condition, the following equation was used.

$$ICR = \frac{(c_a + \sigma_n tan\delta)_{XG}}{(c_a + \sigma_n tan\delta)_{UT}} \quad (4)$$

Based on the above equation calculation results, Fig. 10 demonstrates that at normal pressures less than 50 kPa, XG-BPST improved interface shear strength by at least 10% when compared to the untreated conditions.

## 5. Discussion

This study aimed to apply biopolymer, an eco-friendly material, to improve the soil properties and alleviate environmental issues (carbon neutrality, sustainable development, etc.) associated with the use of cement in geotechnical engineering. When 1 ton of cement is produced, about 1 ton of $CO_2$ is emitted, and geotechnical practices using cement account for 5-8% and 0.2% of global $CO_2$ emissions, respectively (Worrell *et al*. 2001, Metz *et al*. 2005, Chu *et al*. 2009, Oss 2014, Chang *et al*. 2016b, Chang *et al*. 2020). The increasing use of cement has a substantial influence on climate change, leading to a variety of environmental issues such as increased urban water runoff, heat islands, prevention of vegetation growth, and pH (Rao *et al*. 2007, Chang *et al*. 2016b). On the other hand, the production of xanthan gum biopolymer has been reported to consume about 4.97 kg of $CO_2$ per kg, is naturally degradable (biodegradable), and does not adversely affect the geo-environment or groundwater (Chang *et al*. 2016b, Chang *et al*. 2019b). For these reasons, biopolymers have become more popular as alternative materials for reducing cement consumption in geotechnical engineering, particularly as biopolymers can develop higher strength than cement or other binders, even at low concentrations. However, biopolymers are not yet economically competitive with conventional soil binders. Although they are commonly used in other industries that demand high-purity, high-quality biopolymers, they are expensive and uncommon in geotechnical engineering. According to recent reports, the unit prices of XG biopolymers have decreased as the market expands, and the possibility for rough-quality biopolymers to be applied to geotechnical engineering might lead to future competition (Bajaj *et al*. 2007, Chang *et al*. 2015b, Chang *et al*. 2019b). Current biopolymer research is predominantly laboratory-based, and more advanced studies are necessary to develop practical field implementation methodologies, establish design standards, create material quality control guidelines, and ensure the durability and reliability of BPST under site conditions (Chang *et al*. 2020).

MSE wall construction sites with narrow backfill conditions may be difficult to achieve dense compaction using machines, and it may be impossible to secure sufficient geosynthetic length for reinforcement (space restriction). Furthermore, the minimum length of geosynthetic reinforcement materials is commonly determined by the height of the MSE walls, and the pullout resistance is adapted to assess the safety factor for internal stability. Because insufficient reinforcement length affects the stability of MSE walls due to poor pullout resistance, improving mechanical behavior using XG-BPST is an innovative concept. The geogrid layer encapsulated in XG-BPST may resist failures that result in potential slip planes, and the reinforced backfill is anticipated to prevent settlement by increasing bearing capacity.

Fine-grained soils are generally discouraged as backfills for MSE walls owing to their poor drainage, construction challenges, and potential for volume variation and long-term deformations. Furthermore, the poor frictional

resistance of fine-grained backfills might cause reinforcement pullout, reducing the internal stability of MSE walls (Abdi *et al*. 2009, Koerner and Koerner 2018, Ghasemi *et al*. 2024). However, coarse-grained soils are not widely available worldwide and using them in field projects may involve significant procurement and transportation costs. Additionally, there are negative environmental effects owing to aggregate extraction (Mirzaeifar *et al*. 2022, Ok *et al*. 2023). As MSE wall backfill soils can account for up to 50% of the total construction costs, it is estimated that substituting local cohesive soils with construction materials can result in potential savings of 20–30% (Abdi and Arjomand 2011, Mirzaeifar *et al*. 2022). When local cohesive soils used for the MSE wall backfill fail to satisfy the geotechnical requirements, the XG-BPST system may overcome geotechnical challenges by improving engineering performance without the need for chemical additives (e.g., lime or cement).

ASTM D6706 (2021) recommends minimum pullout box dimensions and is intended to be a performance test that simulates design or construction conditions. Large-scale tests are regarded to be more reliable than small-scale tests because they can better replicate the physical structure of reinforced soil and better distribute stresses and strains on the geogrid owing to scale effects (Palmeira 2009). However, large-scale tests have significant drawbacks, including high costs, complex apparatus setup, and lengthy conduct times. Using a small-scale pullout box allows for obtaining soil-geogrid interaction parameters data simply and quickly, with fewer resources. Nonetheless, the scale effect of the pullout box may cause the test results to be unreliable; an appropriate scale effect correction factor can be considered for a more consistent estimate of the interface strength parameters (Barajas *et al*. 2024).

The experimental verification of BPST used in this study is expected to facilitate broader application in geotechnical engineering by overcoming the limitations of current BPST research levels and scale. Although the pullout resistance of the geogrid encapsulated with XG-BPST applied in this study increased significantly, adequate drainage and maintenance are required owing to strength reduction (stability) and durability caused by moist backfill conditions. To address the concern of durability, where XG is susceptible to degradation when exposed to water due to its hydrophilic nature and strength decreases (Soldo *et al*. 2020, Lee *et al*. 2021, Lee *et al*. 2022), studies are being conducted to improve the mechanical performance and durability of XG-BPST by using $Cr^{3+}$ as a crosslinking agent (Lee *et al*. 2023a, Lee *et al*. 2023c). To improve geogrid pullout resistance economically and efficiently using the XG-BPST system, further studies are needed on shortening the construction period (rapid XG drying), determining the optimal BPST type and content, horizontal reinforcement length, vertical reinforcement interval, and after-construction maintenance and repair, and verification of improved soil-geogrid bonding through SEM images.

## 6. Conclusions

This study aimed to enhance the mechanical behavior of reinforced soil structures by introducing the innovative XG-BPST system. Recognizing the nonlinear and complex interface interactions between the geogrid and surrounding soil, critical factors such as backfill characteristics, geogrid geometry and mechanical properties, and applied normal pressure were examined to assess geogrid pullout resistance. A feasibility study was conducted through laboratory pullout tests on reinforced specimens, where geogrids were embedded in sandy soil and encapsulated within a thin XG-BPST layer. The tests were performed using an independently developed apparatus and compared with untreated conditions to assess the system's effectiveness. The main conclusions drawn from the pullout test results are summarized as follows:

The effectiveness of the XG-BPST system in enhancing pullout resistance was validated through the evaluation of interface shear strength parameters (adhesion $c_a$ and average interface friction angle $\delta$) based on the total area method. The apparent friction coefficient served as a comprehensive strength parameter to evaluate the frictional behavior between the geogrid and the surrounding soil. Furthermore, the interaction coefficient ratio (ICR) was employed to quantify the improvement in soil–geogrid interaction resulting from various reinforcement methods.

When the geogrid was encapsulated within the initial (wet) XG-BPST, the peak pullout resistance increased by at least 10% at relatively low normal pressure levels (≤50 kPa). This improvement was attributed to the enhanced shear strength provided by XG hydrogel. However, at higher normal pressure levels, the lubricating effect of the XG hydrogel reduced interface friction and weakened interlocking, leading to negligible variation in pullout resistance from skin friction and bearing resistance. In contrast, under dehydration (dry) conditions, the XG-BPST significantly increased pullout resistance. This was achieved by effectively bonding the soil particles around the geogrid and enhancing particle–geogrid interactions, resulting in improved mechanical behavior of the reinforced soil.

The findings of this study confirm that the XG-BPST system effectively prevents pullout failure in MSE wall backfills under suitable normal pressure conditions. This system is especially beneficial in scenarios where compaction is difficult, where achieving adequate reinforcing length is infeasible due to narrow backfill spaces, or when local fine-grained soils are used. By utilizing eco-friendly materials, the XG-BPST method addresses various geotechnical challenges and offers flexible alternatives for selecting MSE wall backfill materials, making it a sustainable and versatile solution in reinforced soil applications.

## Acknowledgments

This work was supported by the National Research Foundation of Korea (NRF) grant funded by the Korea government (MSIT) (No. 2022R1A2C2091517).

## References


Abdi, M. and Arjomand, M. (2011), "Pullout tests conducted on clay reinforced with geogrid encapsulated in thin layers of sand", *Geotext. Geomembranes*, **29**(6), 588-595. https://doi.org/10.1016/j.geotexmem.2011.04.004.

Abdi, M., Mirzaeifar, H. and Asgardun, Y. (2022), "Novel soil-pegged geogrid (PG) interactions in pull-out loading conditions", *Geotext. Geomembranes*, **50**(4), 764-778. https://doi.org/10.1016/j.geotexmem.2022.04.001.

Abdi, M., Sadrnejad, A. and Arjomand, M. (2009), "Strength enhancement of clay by encapsulating geogrids in thin layers of sand", *Geotext. Geomembranes*, **27**(6), 447-455. https://doi.org/10.1016/j.geotexmem.2009.06.001.

Abdi, M. and Zandieh, A. (2014), "Experimental and numerical analysis of large scale pull out tests conducted on clays reinforced with geogrids encapsulated with coarse material", *Geotext. Geomembranes*, **42**(5), 494-504. https://doi.org/10.1016/j.geotexmem.2014.07.008.

Abdi, M. R., Mirzaeifar, H., Asgardun, Y. and Hatami, K. (2024), "Assessment of pegged geogrid (PG) pullout performance in coarse-grained soils using PIV analysis", *Geotext. Geomembranes*, **52**(1), 27-45. https://doi.org/10.1016/j.geotexmem.2023.09.001.

Aregbesola, S.O. and Byun, Y.H. (2024), "Classification of geogrid reinforcement in aggregate using machine learning techniques", *Int. J. Geo-Eng.*, **15**(1), 4. https://doi.org/10.1186/s40703-024-00206-4.

ASTM (2012), *D3080-04: Standard Test Method for Direct Shear Test of Soils Under Consolidated Drained Conditions*, ASTM International, West Conshohocken, Pennsylvania, U.S.A.

ASTM (2021), *D6706-01: Standard test method for measuring geosynthetic pullout resistance in soil*, ASTM International, West Conshohocken, Pennsylvania, U.S.A.

Bajaj, I.B., Survase, S.A., Saudagar, P.S. and Singhal, R.S. (2007), "Gellan gum: fermentative production, downstream processing and applications", *Food Technol. Biotechnol.*, **45**(4), 341-354.

Barajas, S.R., Pedroso, G.O., Ferreira, F.B. and Lins da Silva, J. (2024), "Influence of apparatus scale on geogrid monotonic and cyclic/post-cyclic pullout behavior in cohesive soils", *Appl. Sci.-Basel*, **14**(13). https://doi.org/10.3390/app14135861.

Becker, A., Katzen, F., Pühler, A. and Ielpi, L. (1998), "Xanthan gum biosynthesis and application: a biochemical/genetic perspective", *Appl. Microbiol. Biotechnol.*, **50**, 145-152. https://doi.org/10.1007/s002530051269.

Bergado, D., Bukkanasuta, A. and Balasubramaniam, A. (1987), "Laboratory pull-out tests using bamboo and polymer geogrids including a case study", *Geotext. Geomembranes*, **5**(3), 153-189. https://doi.org/10.1016/0266-1144(87)90015-X.

Berg, R.R., Christopher, B.R. and Samtani, N.C. (2009a), Design of Mechanically Stabilized Earth Walls and Reinforced Soil Slopes – Volume I. *FHWA*, National Highway Institute Federal Highway Administration U.S. Department of Transportation, Washington, D.C.

Berg, R.R., Christopher, B.R. and Samtani, N.C. (2009b), Design of Mechanically Stabilized Earth Walls and Reinforced Soil Slopes – Volume II. *FHWA*, National Highway Institute Federal Highway Administration U.S. Department of Transportation, Washington, D.C.

Bhowmik, R., Shahu, J. and Datta, M. (2023), "Influence of transverse and longitudinal members of coated polyester-yarn geogrid on pullout response under low normal stress", *Int. J. Civ. Eng.*, **21**(1), 33-50. https://doi.org/10.1007/s40999-022-00741-0.

Cardile, G., Gioffrè, D., Moraci, N. and Calvarano, L. (2017), "Modelling interference between the geogrid bearing members under pullout loading conditions", *Geotext. Geomembranes*, **45**(3), 169-177. https://doi.org/10.1016/j.geotexmem.2017.01.008.

Chang, I. and Cho, G.-C. (2012), "Strengthening of Korean residual soil with β-1, 3/1, 6-glucan biopolymer", *Constr. Build. Mater.*, **30**, 30-35. https://doi.org/10.1016/j.conbuildmat.2011.11.030.

Chang, I. and Cho, G.C. (2019), "Shear strength behavior and parameters of microbial gellan gum-treated soils: from sand to clay", *Acta Geotech.*, **14**, 361-375. https://doi.org/10.1007/s11440-018-0641-x.

Chang, I., Im, J. and Cho, G.C. (2016a), "Geotechnical engineering behaviors of gellan gum biopolymer treated sand", *Can. Geotech. J*, **53**(10), 1658-1670. https://doi.org/10.1139/cgj-2015-0475.

Chang, I., Im, J. and Cho, G.C. (2016b), "Introduction of microbial biopolymers in soil treatment for future environmentally-friendly and sustainable geotechnical engineering", *Sustainability*, **8**(3), 251. https://doi.org/10.3390/su8030251.

Chang, I., Im, J., Prasidhi, A.K. and Cho, G.C. (2015a), "Effects of Xanthan gum biopolymer on soil strengthening", *Constr. Build. Mater.*, **74**, 65-72. https://doi.org/10.1016/j.conbuildmat.2014.10.026.

Chang, I., Kwon, Y.M., Im, J. and Cho, G.C. (2019a), "Soil consistency and interparticle characteristics of xanthan gum biopolymer–containing soils with pore-fluid variation", *Can. Geotech. J.*, **56**(8), 1206-1213. https://doi.org/10.1139/cgj-2018-0254.

Chang, I., Lee, M. and Cho, G.C. (2019b), "Global CO2 emission-related geotechnical engineering hazards and the mission for sustainable geotechnical engineering", *Energies*, **12**(13), https://doi.org/10.3390/en12132567.

Chang, I., Lee, M., Tran, A.T.P., Lee, S., Kwon, Y.M., Im, J. and Cho, G.C. (2020), "Review on biopolymer-based soil treatment (BPST) technology in geotechnical engineering practices", *Transp. Geotech.*, **24**, 100385. https://doi.org/10.1016/j.trgeo.2020.100385.

Chang, I., Prasidhi, A.K., Im, J. and Cho, G.C. (2015b), "Soil strengthening using thermo-gelation biopolymers", *Constr. Build. Mater.*, **77**, 430-438. https://doi.org/10.1016/j.conbuildmat.2014.12.116.

Choi, S.G., Chang, I., Lee, M., Lee, J.H., Han, J.T. and Kwon, T.H. (2020), "Review on geotechnical engineering properties of sands treated by microbially induced calcium carbonate precipitation (MICP) and biopolymers", *Constr. Build. Mater.*, **246**, 118415. https://doi.org/10.1016/j.conbuildmat.2020.118415.

Chu, J., Varaksin, S., Klotz, U. and Mengé, P. (2009), "Construction processes", *Proceedings of the 17th International Conference on Soil Mechanics and Geotechnical Engineering*, **1-4**, IOS Press, 3006-3135. 10.3233/978-1-60750-031-5-3006.

Christopher, B.R. and Stulgis, R.P. (2005), "Low permeable backfill soils in geosynthetic reinforced soil walls: State-of-the-practice in North America", *Proceedings of North American geo-synthetics conference (NAGS 2005)*, 14-16.

Derksen, J., Ziegler, M. and Fuentes, R. (2021), "Geogrid-soil interaction: A new conceptual model and testing apparatus", *Geotext. Geomembranes*, **49**(5), 1393-1406. https://doi.org/10.1016/j.geotexmem.2021.05.011.

Esfandiari, J. and Selamat, M. (2012), "Laboratory investigation on the effect of transverse member on pull out capacity of metal strip reinforcement in sand", *Geotext. Geomembranes*, **35**, 41-49. https://doi.org/10.1016/j.geotexmem.2012.07.002.

Gao, Y., Hang, L., He, J., Zhang, F. and Van Paassen, L. (2021), "Pullout behavior of geosynthetic reinforcement in biocemented soils", *Geotext. Geomembranes*, **49**(3), 646-656. https://doi.org/10.1016/j.geotexmem.2020.10.028.

Garcıa-Ochoa, F., Santos, V., Casas, J. and Gómez, E. (2000), "Xanthan gum: production, recovery, and properties", *Biotechnol. Adv.*, **18**(7), 549-579. https://doi.org/10.1016/S0734-9750(00)00050-1.

Ghasemi, S.M., Binesh, S.M. and Shourijeh, P.T. (2024), "Improving clay-geogrid interaction: Enhancing pullout resistance with recycled concrete aggregate encapsulation", *Geotext. Geomembranes*, **52**(6), 1145-1160. https://doi.org/10.1016/j.geotexmem.2024.07.010.

Hataf, N. and Sadr, A. (2015), "Experimental, numerical and analytical study on conventional and innovative Grid-Anchor system in the pull-out test", *Geotext. Geomembranes*, **10**(3), 182-193. https://doi.org/10.1080/17486025.2014.933893.

Horpibulsuk, S. and Niramitkornburee, A. (2010), "Pullout resistance of bearing reinforcement embedded in sand", *Soils Found.*, **50**(2), 215-226. https://doi.org/10.3208/sandf.50.215.

Jain, S., Mishra, P.N., Tiwari, S., Wang, Y., Jiang, N., Dash, H.R., Chang, I., Kumar, A., Das, S.K., Scheuermann, A. and Bore, T. (2023), "Biological perspectives in geotechnics: theoretical developments", *Rev. Environ. Sci. Bio-Technol.*, **22**(4), 1093-1130. https://doi.org/10.1007/s11157-023-09671-2.

Jewell, R.A. (1996), *Soil Reinforcement with Geotextile*, CIRIA Thomas Telford, London.

Khedkar, M. and Mandal, J. (2009), "Pullout behaviour of cellular reinforcements", *Geotext. Geomembranes*, **27**(4), 262-271. https://doi.org/10.1016/j.geotexmem.2008.12.003.

Koerner, R.M. and Koerner, G.R. (2018), "An extended data base and recommendations regarding 320 failed geosynthetic reinforced mechanically stabilized earth (MSE) walls", *Geotext. Geomembranes*, **46**(6), 904-912. https://doi.org/10.1016/j.geotexmem.2018.07.013.

Lee, M., Chang, I. and Cho, G.C. (2023a), "Advanced biopolymer–based soil strengthening binder with trivalent chromium–Xanthan gum crosslinking for wet strength and durability enhancement", *J. Mater. Civ. Eng.*, **35**(10), 04023360. https://doi.org/10.1061/JMCEE7.MTENG-16123.

Lee, M., Chang, I., Kang, S.J., Lee, D.H. and Cho, G.C. (2023b), "Alkaline induced-cation crosslinking biopolymer soil treatment and field implementation for slope surface protection", *Geomech. Eng*, **33**(1), 29-40. https://doi.org/10.12989/gae.2023.33.1.029.

Lee, M., Chang, I., Park, D.Y. and Cho, G.C. (2023c), "Strengthening and permeability control in sand using Cr3+-crosslinked xanthan gum biopolymer treatment", *Transp. Geotech.*, **43**, 101122. https://doi.org/10.1016/j.trgeo.2023.101122.

Lee, M., Im, J., Cho, G.C., Ryu, H.H. and Chang, I. (2021), "Interfacial shearing behavior along Xanthan gum biopolymer-treated sand and solid interfaces and its meaning in geotechnical engineering aspects", *Appl. Sci.-Basel*, **11**(1), 139. https://doi.org/10.3390/app11010139.

Lee, M., Kwon, Y.M., Park, D.Y., Chang, I. and Cho, G.C. (2022), "Durability and strength degradation of xanthan gum based biopolymer treated soil subjected to severe weathering cycles", *Sci. Rep.*, **12**(1), 19453. https://doi.org/10.1038/s41598-022-23823-4.

Lee, S., Chang, I., Chung, M.K., Kim, Y. and Kee, J. (2017), "Geotechnical shear behavior of xanthan gum biopolymer treated sand from direct shear testing", *Geomech. Eng.*, **12**(5), 831-847. https://doi.org/10.12989/gae.2017.12.5.831.

Maleki, A., Lajevardi, S., Briançon, L., Nayeri, A. and Saba, H. (2021), "Experimental study on the L-shaped anchorage capacity of the geogrid by the pullout test", *Geotext. Geomembranes*, **49**(4), 1046-1057. https://doi.org/10.1016/j.geotexmem.2021.02.003.

Metz, B., Davidson, O., De Coninck, H., Loos, M. and Meyer, L. (2005), "IPCC special report on carbon dioxide capture and storage", Cambridge: Cambridge University Press.

Mirzaalimohammadi, A., Ghazavi, M., Roustaei, M. and Lajevardi, S.H. (2019), "Pullout response of strengthened geosynthetic interacting with fine sand", *Geotext. Geomembranes*, **47**(4), 530-541. https://doi.org/10.1016/j.geotexmem.2019.02.006.

Mirzaeifar, H., Hatami, K. and Abdi, M.R. (2022), "Pullout testing and Particle Image Velocimetry (PIV) analysis of geogrid reinforcement embedded in granular drainage layers", *Geotext. Geomembranes*, **50**(6), 1083-1109. https://doi.org/10.1016/j.geotexmem.2022.06.008.

Moraci, N., Cardile, G., Gioffrè, D., Mandaglio, M.C., Calvarano, L.S. and Carbone, L. (2014), "Soil geosynthetic interaction: design parameters from experimental and theoretical analysis", *Transp. Infrastruct. Geotechnol.*, **1**, 165-227. https://doi.org/10.1007/s40515-014-0007-2.

Moraci, N. and Gioffrè, D. (2006), "A simple method to evaluate the pullout resistance of extruded geogrids embedded in a compacted granular soil", *Geotext. Geomembranes*, **24**(2), 116-128. https://doi.org/10.1016/j.geotexmem.2005.11.001.

Moraci, N. and Recalcati, P. (2006), "Factors affecting the pullout behaviour of extruded geogrids embedded in a compacted granular soil", *Geotext. Geomembranes*, **24**(4), 220-242. https://doi.org/10.1016/j.geotexmem.2006.03.001.

Namjoo, A.M., Soltani, F. and Toufigh, V. (2021), "Effects of moisture on the mechanical behavior of sand–geogrid: an experimental investigation", *Int. J. Geosynth. Ground Eng.*, **7**, 1-13. https://doi.org/10.1007/s40891-020-00243-w.

Ochiai, H., Otani, J., Hayashic, S. and Hirai, T. (1996), "The pull-out resistance of geogrids in reinforced soil", *Geotext. Geomembranes*, **14**(1), 19-42. https://doi.org/10.1016/0266-1144(96)00027-1.

Ok, B., Colakoglu, H., and Dagli, U. (2023), "Evaluation of the geogrid-various sustainable geomaterials interaction by direct shear tests", *Geomech. Eng.*, **34**(2), 173-186. https://doi.org/10.12989/gae.2023.34.2.173.

Oss, H. (2014), "Cement statistics and Information", US Geological Survey: Reston, VA, USA.

Palmeira, E.M. (2009), "Soil–geosynthetic interaction: Modelling and analysis", *Geotext. Geomembranes*, **27**(5), 368-390. https://doi.org/10.1016/j.geotexmem.2009.03.003.

Pant, A., Datta, M., Ramana, G. and Bansal, D. (2019), "Measurement of role of transverse and longitudinal members on pullout resistance of PET geogrid", *Measurement*, **148**, 106944. https://doi.org/10.1016/j.measurement.2019.106944.

Pant, A. and Ramana, G. (2022), "Prediction of pullout interaction coefficient of geogrids by extreme gradient boosting model", *Geotext. Geomembranes*, **50**(6), 1188-1198. https://doi.org/10.1016/j.geotexmem.2022.08.003.

Rao, A., Jha, K.N. and Misra, S. (2007), "Use of aggregates from recycled construction and demolition waste in concrete", *Resour. Conserv. Recycl.*, **50**(1), 71-81. https://doi.org/10.1016/j.resconrec.2006.05.010.

Razeghi, H.R. and Ensani, A. (2023), "Clayey sand soil interactions with geogrids and geotextiles using large-scale direct shear tests", *Int. J. Geosynth. Ground Eng.*, **9**(2), 24. https://doi.org/10.1007/s40891-023-00443-0.

Sadat Taghavi, S. and Mosallanezhad, M. (2017), "Experimental analysis of large-scale pullout tests conducted on polyester anchored geogrid reinforcement systems", *Can. Geotech. J.*, **54**(5), 621-630. https://doi.org/10.1139/cgj-2016-0365.

Sieira, A.C.C.F., Gerscovich, D.M.S. and Sayão, A.S.F.J. (2009), "Displacement and load transfer mechanisms of geogrids under pullout condition", *Geotext. Geomembranes*, **27**(4), 241-253. https://doi.org/10.1016/j.geotexmem.2008.11.012.

Shin, E. and Yun, S. (2003), "Friction features of geosynthetics through the pullout test", *J. Korean Geosynth. Soc.*, **2**(1), 3-13.

Soldo, A., Miletić, M. and Auad, M. L. (2020), "Biopolymers as a sustainable solution for the enhancement of soil mechanical properties", *Sci. Rep.*, **10**(1), 267. 10.1038/s41598-019-57135-x.

Stokes, J.R., Macakova, L., Chojnicka-Paszun, A., de Kruif, C.G. and de Jongh, H.H. (2011), "Lubrication, adsorption, and rheology of aqueous polysaccharide solutions", *Langmuir*, **27**(7), 3474-3484. https://doi.org/10.1021/la104040d.

Teixeira, S.H., Bueno, B.S. and Zornberg, J.G. (2007), "Pullout resistance of individual longitudinal and transverse geogrid ribs", *J. Geotech. Geoenviron. Eng.*, **133**(1), 37-50. https://doi.org/10.1061/(ASCE)1090-0241(2007)133:1(37).

Wang, Z., Jacobs, F. and Ziegler, M. (2016), "Experimental and DEM investigation of geogrid–soil interaction under pullout loads", *Geotext. Geomembranes*, **44**(3), 230-246. https://doi.org/10.1016/j.geotexmem.2015.11.001.

Wang, Z., Xia, Q., Yang, G., Zhang, W. and Zhang, G. (2023), "Effects of transverse members on geogrid pullout behavior considering rigid and flexible top boundaries", *Geotext. Geomembranes*, **51**(4), 72-84. https://doi.org/10.1016/j.geotexmem.2023.03.005.

Worrell, E., Price, L., Martin, N., Hendriks, C. and Meida, L.O. (2001), "Carbon dioxide emissions from the global cement industry", *Annu. Rev. Environ. Resour.*, **2**, 303-329. https://doi.org/10.1146/annurev.energy.26.1.303.

Yang, K.H., Thuo, J., Chen, J.W. and Liu, C.N. (2019), "Failure investigation of a geosynthetic-reinforced soil slope subjected to rainfall", *Geosynth. Int*, **26**(1), 42-65. https://doi.org/10.1680/jgein.18.00035.

Zamani, S., Lajevardi, S.H., Yarivand, A. and Zeighami, E. (2023), "Experimental study of the behavior of square footing on reinforced sand with treated geotextile", *Int. J. Geo-Eng.*, **14**(1), 19. https://doi.org/10.1186/s40703-023-00195-w.